WSU-HEP-1706, MI-TH-1748

Heavy Neutrino Search via the Higgs boson at the LHC

Arindam Das,[1,2,3,*] Yu Gao,[4,†] and Teruki Kamon[5,‡]

[1]*School of Physics, KIAS, Seoul 130-722, Korea*

[2]*Department of Physics & Astronomy,*
Seoul National University 1 Gwanak-ro, Gwanak-gu, Seoul 08826, Korea

[3]*Korea Neutrino Research Center, Bldg 23-312,*
Seoul National University, Sillim-dong, Gwanak-gu, Seoul 08826, Korea

[4]*Department of Physics and Astronomy,*
Wayne State University, Detroit, 48201, USA

[5] *Mitchell Institute for Fundamental Physics and Astronomy,*
Department of Physics and Astronomy,
Texas A&M University, College Station, TX 77843-4242, USA

arXiv:1704.00881v1 [hep-ph] 4 Apr 2017

Abstract

In inverse see-saw the effective neutrino Yukawa couplings can be sizable due to a large mixing angle. When the right-handed neutrino (N) is lighter than the Higgs boson (h), it can be produced via the on-shell decay of an Higgs boson at the LHC. The Standard Model (SM) Higgs boson offers an opportunity to probe the neutrino mixing. In this paper we adopt N below the Higgs mass, and found the QCD dominated $pp \to hj$ channel can lead to a signal by singly producing N at the LHC. In such a process, the SM Higgs boson can decay via $h \to N\nu$ at a significant branching fraction, and the N mass can be reconstructed in its dominant semilpetonic decays. We perform an analysis on this channel and its relevant backgrounds, among which the W+jets background is the largest. Considering the existing mixing constraints from Higgs and electroweak precision data, the best sensitivity of the heavy neutrino search is found to be in the 100- 110 GeV range at the upcoming high luminosity runs.

PACS numbers:

Keywords: Heavy Neutrino Search, Higgs boson Data, New Production Channel, Collider Phenomenology

*Electronic address: arindam@kias.re.kr

†Electronic address: yugao@wayne.edu

‡Electronic address: kamon@physics.tamu.edu

Contents

I. Introduction 3

II. Bounds on the Mixings 5

III. Higgs boson + jet cross-sections 9

IV. Collider Signals and Backgrounds 12

V. Conclusion 16

References 17

I. INTRODUCTION

The existence of the tiny neutrino mass and the flavor mixing have been observed by the recent neutrino oscillation experiments [1–6] which requires us to extend the Standard Model (SM). Among the different extensions of the SM, the seesaw or type-I seesaw mechanism [7–13] is the probably the simplest idea to naturally explain the tiny neutrino mass. Due to the variation of the seesaw scale form the intermediate scale to the electroweak scale, the neutrino Dirac Yukawa coupling (Y_D) varies from scale of the electron Yukawa coupling to the top quark Yukawa coupling. Being SM gauge singlets, the right handed (RH) heavy Majorana neutrinos interact with the SM gauge bosons through the Dirac Yukawa coupling. The heavy neutrinos in the TeV or GeV scale, employed by the seesaw mechanism, have too small Dirac Yukawa coupling $\sim \mathcal{O}(10^{-6})$ to produce the observable signatures at the high energy colliders such as Large Hadron Collider (LHC) and Linear Collider (LC).

There is another type of seesaw mechanism, commonly known as the inverse seesaw mechanism [14–16] where a small neutrino mass is generated by a tiny lepton number violating parameter. Where in case of seesaw mechanism a large lepton number violating mass term is introduced as a suppression factor to produce the tiny neutrino mass. In case of inverse seesaw, the heavy neutrinos are pseudo-Dirac particles with $Y_D \sim \mathcal{O}(1)$ so that such RH neutrinos could be produced at the LHC and LC while having masses in the TeV or GeV scale. The relevant particle content of the model is given by Tab. I

	SU(2)	$U(1)_Y$
ℓ_L	**2**	$-1/2$
H	**2**	$+1/2$
N_R	**1**	0
S_L	**1**	0

TABLE I: Partcile quantum numbers in the inverse seesaw extension of the SM.

The relevant part of the Lagrangian is given by [1]

$$\mathcal{L} \supset -Y_D^{\alpha\beta}\overline{\ell_L^\alpha}\tilde{H}N_R^\beta - M_N^{\alpha\beta}\overline{S_L^\alpha}N_R^\beta - \frac{1}{2}\mu_{\alpha\beta}\overline{S_L^\alpha}S_L^{\beta C} + H.c., \tag{1}$$

[1] It is crucial in inverse seesaw to forbid the Majorana mass term for N_R. For realization in the next-to-minimal supersymmetryic SM, see [17]

where N_R and S_L are two SM-singlet heavy neutrinos with the same lepton numbers, ℓ_L is the SM lepton doublet, H is the SM Higgs doublet, α, β are the lepton flavor indices, m_N is the Dirac mass matrix and μ is a small Majorana mass matrix violating the lepton numbers.

The neutrino mass matrix is

$$M_\nu = \begin{pmatrix} 0 & m_D & 0 \\ m_D^T & 0 & M_N^T \\ 0 & M_N & \mu \end{pmatrix}. \tag{2}$$

Diagonalizing this mass matrix we obtain the light neutrino mass matrix

$$m_\nu \simeq (m_D M_N^{-1})\mu(M_N^{-1^T} m_D^T) \tag{3}$$

where $m_D = Y_D \frac{v}{\sqrt{2}}$. Note that the smallness of the light neutrino mass originates from the small lepton number violating term μ. The smallness of μ allows the $m_D M_N^{-1}$ parameter to be order one even for an electroweak scale heavy neutrino. Since the scale of μ is much smaller than the scale of M_N, the heavy neutrinos become the pseudo-Dirac particles.

We consider a flavor-diagonal m_D and M_N structure of μ, where there is no mixing between different flavors of heavy neutrinos. An explicit numerical fit is given in [19]. Due to flavor dependence in electroweak precision constraints, in this paper we consider two benchmark scenarios. One is the 'Single Flavor' (SF) case, where only one flavor heavy pseudo-Dirac pair resides at the electroweak scale whereas the other flavors' heavy pairs are beyond reach of the LHC. Here we consider such a SF cases for electron and muon type neutrinos, respectively. For an alternative scenario, we also consider the 'Flavor Diagonal' (FD) case that both the first two flavor (electron and muon) heavy pseudo-Dirac pairs are at the weak scale , while those for the thrid flavor are heavy. For simplicity we assume the (electron and muon) flavor N have the same mass.

Our paper is arranged in the following way. In Sec. II we discuss the recent experimental bounds on the heavy neutrino searches. In Sec. III we discuss about the $h + j$ production and the subsequent decay of the Higgs boson into the heavy neutrino. We also describe the different decay modes of the heavy neutrino. In Sec. IV we study the complete collider study of the signal and the SM backgrounds. Sec. V is dedicated for the conclusion.

II. BOUNDS ON THE MIXINGS

Being SM gauge singlets, the heavy mass eigenstate of neutrinos can interact with the W and Z bosons via its mixings into the SM neutrino, as

$$\nu \simeq \nu_m + V_{\ell N} N_m, \tag{4}$$

where $V_{\ell N}$ is the mixing between the SM neutrino and the SM gauge singlet RH heavy neutrino assuming $|V_{\ell N}| \ll 1$. Here ν is the flavor eigenstate whereas ν_m and N_m are corresponding light heavy mass eigenstates respectively. For convenience in notation, from now on we also use N to denote the heavy mass eigenstate without further notice.

The charged current (CC) and neutral current (NC) interactions can be expressed in terms of the mass eigenstates of the light-RH neutrinos as

$$\mathcal{L}_{CC} \supset -\frac{g}{\sqrt{2}} W_\mu \bar{e} \gamma^\mu P_L V_{\ell N} N + \text{h.c.}, \tag{5}$$

where e denotes the three generations of the charged leptons, and $P_L = \frac{1}{2}(1-\gamma_5)$ is the projection operator. Similarly, in terms of the mass eigenstates the neutral current interaction is written as

$$\mathcal{L}_{NC} \supset -\frac{g}{2c_w} Z_\mu \left[\overline{N} \gamma^\mu P_L |V_{\ell N}|^2 N + \{ \overline{\nu_m} \gamma^\mu P_L V_{\ell N} N + \text{h.c.} \} \right], \tag{6}$$

where $c_w = \cos\theta_w$ with θ_w being the weak mixing angle. We notice from Eqs. 1, 5 and 6 that the production cross section of the heavy neutrinos in association with a lepton or SM light neutrino is proportional to $|V_{\ell N}|^2$. However, the Yukawa coupling in Eq. 1 can also be directly measured from the decay mode of the Higgs boson such as $h \to N\nu$ applying the bounds obtained from invisible Higgs boson decay widths. The recent and the projected bounds on the mixing angle as a function of M_N from different experiments are shown in Fig. 1.

For $M_N < M_Z$, the heavy neutrino can be produced from the Z-decay through through the NC interaction with missing energy. The heavy neutrino can decay according CC and NC interactions. Such processes have been discussed in [18, 20]. In [20–22], a scale dependent production cross section at the Leading Order (LO) and Next-to-Leading-Oder QCD (NLO QCD) of $N\nu$ at the LO and NLO have been studied at the 14 TeV LHC and 100 TeV hadron collider. The L3 collaboration [23] has performed a search on such heavy neutrinos directly from the LEP data and found a limit on $\mathcal{B}(Z \to \nu N) < 3 \times 10^{-5}$ at the 95% CL for the mass range up to 93 GeV. The exclusion limits from L3 are given in Fig. 1 where the red dot-dashed

line stands for the limits obtained from electron (L3-e) and the red dashed line stands for the exclusion limits coming from μ (L3-μ). The corresponding exclusion limits on $|V_{(\ell=e)N}|$at the 95% CL [24, 25] have been drawn from the LEP2 data which have been denoted by the dark magenta line. In this analysis they searched for 80 GeV $\leq$ M$_N$ $\leq$ 205 GeV with a center of mass energy between 130 GeV to 208 GeV [25].

The DELPHI collaboration [26] had also performed the same search from the LEP-I data which set an upper limit for the branching ratio $\mathcal{B}(Z \to N\nu)$ about 1.3×10^{-6} at 95% CL for 3.5 GeV $\leq M_N \leq$ 50 GeV. Outside this range the limit starts to become weak with the increase in M_N. In both of the cases they have considered $N \to W\ell$ and $N \to Z\nu$ decays after the production of the heavy neutrino was produced. The exclusion limits for $\ell = e, \mu, \tau$ are depicted by the blue dotted, dashed and dot-dashed lines in Fig. 1.

The search of the sterile neutrinos can be made at high energy lepton colliders with a very high luminosity such as Future Circular Collider (FCC) for the seesaw model. A design of such collider has been launched recently where nearly 100 km tunnel will be used to study high luminosity e^+e^- collision (FCC-ee) with a center-of-mass energy around 90 GeV to 350 GeV [27]. According to this report, a sensitivity down to $|V_{\ell N}|^2 \sim 10^{-11}$ could be achieved from a range of the heavy neutrino mass, 10 GeV $\leq M_N \leq$ 80 GeV. The darker cyan-solid line in Fig. 1 shows the prospective search reaches by the FCC-ee. A sensitivity down to a mixing of $|V_{\ell N}|^2 \sim 10^{-12}$ can be obtained in FCC-ee [27], covering a large phase space for M_N from 10 GeV to 80 GeV.

The heavy neutrinos can participate in many electroweak (EW) precision tests due to the active-sterile couplings. For comparison, we also show the 95% CL indirect upper limit on the mixing angle, $|V_{\ell N}| < 0.030, 0.041$ and 0.065 for $\ell = \mu, e, \tau$ respectively derived from a global fit to the electroweak precision data (EWPD), which is independent of M_N for $M_N > M_Z$, as shown by the horizontal pink dash, solid and dolled lines respectively in Fig. 1 [28–30]. For the mass range, $M_N < M_Z$, it is shown in [31] that the exclusion limit on the mixing angle remains almost unaltered, however, it varies drastically at the vicinity of $M_N = 1$ GeV. For the flavor universal case the bound on the mixing angle is given as $|V_{\ell N}|^2 = 0.025$ from [28] which has been depicted in Fig. 1 with a pink dot-dashed line.

The relevant existing upper limits at the 95% CL are also shown to compare with the experimental bounds using the LHC Higgs boson data in [32, 33] using [34–38]. The darker green dot-dashed line named Higgs boson shows the relevant bounds on the mixing angle. In this analysis we will compare our results taking this line as one of the references. We have

noticed that the $|V_{\ell N}|^2$ can be as low as 4.86×10^{-4} while $M_N = 60$ GeV and the bound becomes stronger at $M_N = 100$ GeV as 3.73×10^{-4}. When $M_N > 100$ GeV, the bounds on $|V_{\ell N}|^2$ become weaker.

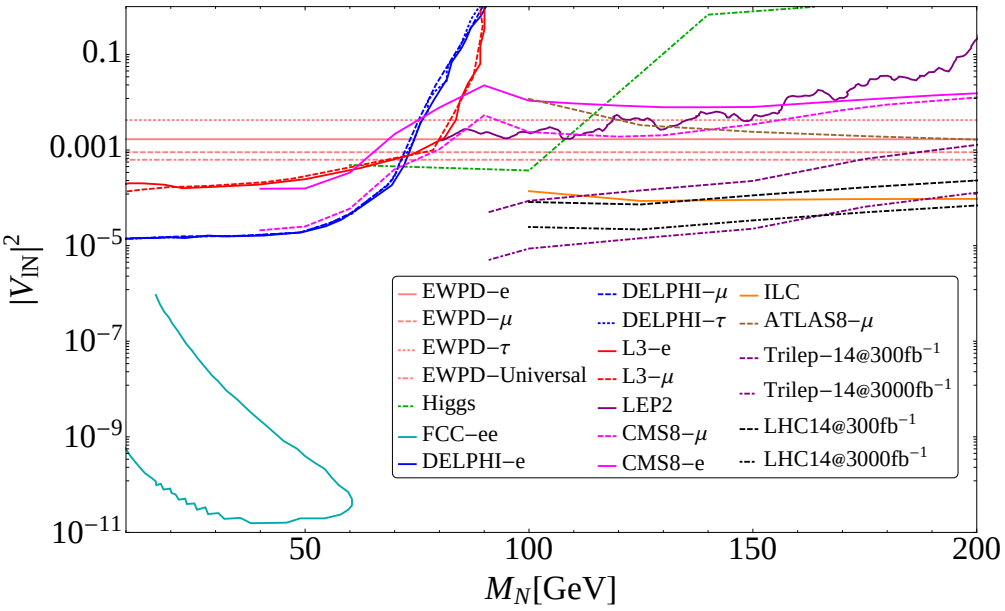

FIG. 1: Experimental and prospective upper bounds on $|V_{\ell N}|^2$ as a function of M_N.

The prospective bounds on $|V_{eN}|^2$ from the e^+e^- linear collider at $\sqrt{s} = 500$ GeV with a 500 fb^{-1} luminosity has been studied in [39] where the analysis could probe down to 10^{-4} taking 100 GeV $\leq$ M$_N$ $\leq$ 500GeV. The solid orange line represents the prospective bounds at ILC.

LHC has also performed the direct searches on the Majorana heavy neutrinos. The ATLAS detector at the 7 TeV with a luminosity of 4.9 fb^{-1} [40] studied the $\mu^\pm\mu^\pm$+jets in the type-I seesaw model framework for 100 GeV $\leq M_N \leq$ 500 GeV. They have interpreted the limit in terms of the mixing angle, $|V_{(\ell=\mu)N}|^2$ which is shown in the Fig. 1. The corresponding bounds for the μ at the 8 TeV with a luminosity of 20.3 fb^{-1} [41] is interpreted as the dashed darker cyan line as ATLAS8-μ in the same figure.[2]

The CMS also studied the type-I seesaw model from the $e^\pm e^\pm$+jets and $\mu^\pm\mu^\pm$+jets final states in [42] at the 8 TeV LHC with a luminosity of 19.7 fb^{-1} with 30 GeV$\leq M_N \leq$ 500 GeV. The limits from the CMS in the for μ is roughly comparable to the DELPHI result while $M_N < 70$ GeV. The CMS limits are denoted by CMS8-e and CMS8-μ with the magenta

[2] The weaker bounds at the 7 TeV ATLAS are not shown in Fig. 1, however, the bounds can be read from [40].

dashed and solid lines respectively.

Using such limits, in [43] the prospective bounds on $|V_{\ell N}|^2$ at the 14 TeV LHC with 300 fb^{-1} (black, dott dashed line LHC14@300 fb^{-1}) and 3000 fb^{-1} luminosities are given for the type-I seesaw case for 91.2 GeV $\leq M_N \leq$ 500 GeV. The prospective bounds for the type-I seesaw case could be better than the ILC bounds while the LHC luminosity will be 3000 fb^{-1}(black, dotted line LHC14@3000 fb^{-1}) and at that point the mixing angle could be probed down to 10^{-5}. The range of the mixing angles for the type-I seesaw case using the lepton flavor violation bounds and general parameterizations have been studied in [44] for the type-I seesaw case using two generations of the degenerate heavy neutrinos having masses around 100 GeV.

In [43] the prospective upper bounds on $|V_{(\ell=e,\mu)N}|^2$ have been obtained studying the trilepton plus missing energy final state using the inverse seesaw model at the 14 TeV LHC with a luminosity of 300 fb^{-1}(dark purple, dashed line Trilep-14@300 fb^{-1}) and 3000 fb^{-1}(dark purple, dot-dashed line Trilep-14@3000 fb^{-1}). At the 300 fb^{-1} luminosity $|V_{\ell N}|^2$ could be probed down to $\mathcal{O}(10^{-5})$ where as a luminosity of 3000 fb^{-1} can make it better by two orders of magnitude. In Eq. 6, there is a part where the heavy neutrino can produced in a pair from the NC interaction where the production cross section will be proportional to $|V_{\ell N}|^4$. A detailed scale dependent LO and NLO-QCD studies of this process followed by various multilepton decays of the heavy neutrino have been studied in [45]. It is shown that 95 GeV$\leq M_N \leq$ 160 GeV could be probed well at the high energy colliders at very high luminosity while the results will be better than the results from EWPD.

In this work we will consider on 20 GeV $\leq M_N \leq$ 120 GeV where the heavy neutrino will be produced from the on-shell decay of the Higgs boson. Therefore we chose the Higgs boson line for the mixing angles and also picked up some 'benchmark' values of the mixing angles $|V_{\ell N}|^2 = 10^{-3}$ to 10^{-8} which are favored by the current and prospective bounds. It must be clarified that on-shell decay of the Higgs boson into $N\nu$ will show same repertoire for the Majorana type, pseudo-Dirac type and Dirac type heavy neutrinos irrespective of the models, provided that N is lighter than the Higgs boson. In the mixing angles values, $|V_{\ell N}|^2 = 10^{-7}$ and 10^{-8} range are also shown for a future 100 TeV pp collider, where such a small mixing can be potentially probed.

III. HIGGS BOSON + JET CROSS-SECTIONS

The Higgs boson can decay into a right handed pseudo-Dirac heavy neutrino and a SM neutrino via the $\nu - N$ mixing. If M_N lies between 40 GeV− 120 GeV, the Higgs boson can decay on-shell into the RH neutrino through a single production channel shown in Fig. 2.

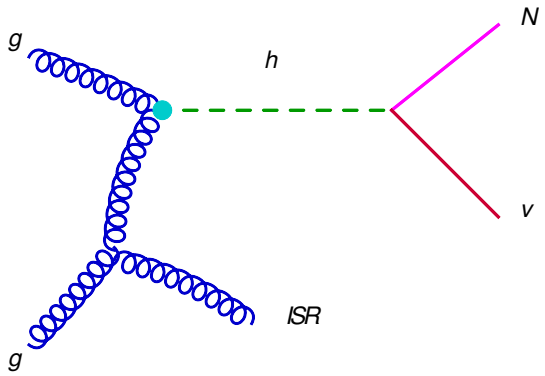

FIG. 2: Production of the heavy neutrino via Higgs boson decay associated with an ISR jet.

The Higgs boson's SM decay width is taken as $\Gamma_h^{\rm SM} = 4.1$ MeV, with allowance to fit in BSM physics where the Higgs boson can decay into the SM singlet RH heavy neutrino in association with missing energy. The partial decay width is given by

$$\Gamma(h \to N\nu) = \frac{Y_N^2}{8\pi m_h^3}(m_h^2 - M_N^2)^2 \tag{7}$$

and it sums $h \to N\overline{\nu}$ and $h \to \overline{N}\nu$ cases. The branching fraction of the Higgs boson to the heavy neutrino is

$$\mathcal{B}_{h\to N\nu} = \frac{\Gamma(h \to N\nu)}{\Gamma_h^{\rm SM} + \Gamma(h \to N\nu)} \tag{8}$$

We focus on the signal channel of single Higgs boson production[3] with an associated jet, and utilize the consequent decay of the Higgs boson. The inclusion of an extra jet is necessary due to the requirement of experimentally triggering on the event, and also due to the fact that most of the Higgs boson decay products are not very energetic without a transverse boost from the associated initial state jet.

The $pp \to hj$ production cross-section at 13 TeV has been studied to the next-next-to-leading order (NNLO) in [47, 48], and we adopt the results wherein,

$$\sigma(h + j)_{\rm LO} \;=\; 1.1 \text{ pb}$$

[3] In the FD case, $\mathcal{B}_{h\to N\nu} = \frac{2\Gamma(h\to N\nu)}{\Gamma_h^{\rm SM}+2\Gamma(h\to N\nu)}$

$$\sigma(h+j)_{\rm NLO} \;=\; 1.6 \text{ pb}$$
$$\sigma(h+j)_{\rm NNLO} \;=\; 1.9 \text{ pb} \tag{9}$$

with a jet transverse momentum, $p_T^j > 100$ GeV. Here we increase the leading p_T^j requirement to reduce the amount of background, as well as to distinguish the ISR jet from the jets from N decays, as will be discussed in the following section. Including the Higgs boson decay branching ratios, the signal cross-section for a single heavy neutrino can be written as

$$\sigma = \sigma(h+j)\mathcal{B}_{h\to N\nu} \tag{10}$$

depending upon M_N, the production cross section of the heavy neutrino is shown in Fig. 3 at 13 TeV LHC, for ISR jet $p_T^j > 100$ GeV.

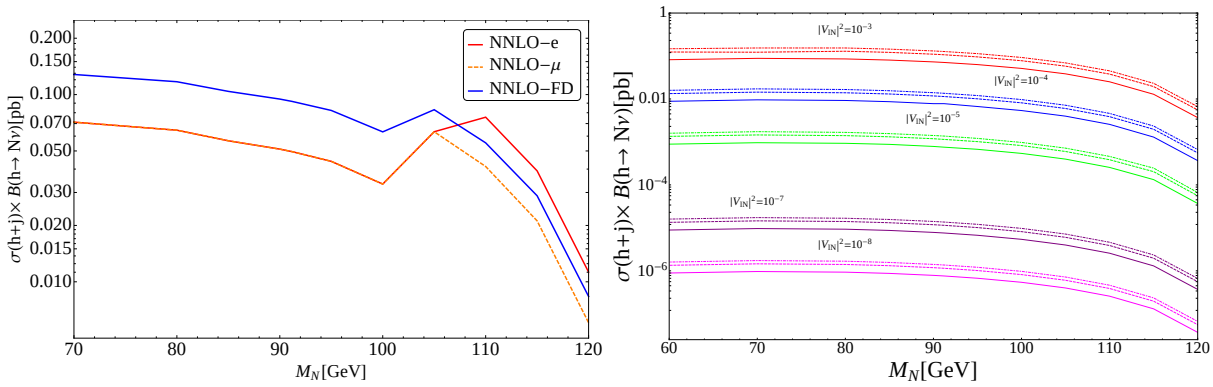

FIG. 3: Upper bounds on the production cross sections of $N\nu$ from $h+j$ process with maximally allowed mixing angles from [28, 32, 33]. The electron and muon flavor curves deviate due to different EWPD constraints. The hj production is shown at the NNLO level in the left panel. The right panel shows the SF signal cross-section at fixed mixing angle values, with $p_T^j > 100$ GeV at $\sqrt{s} = 13$ TeV. For the FD case, the signal cross-section doubles.

To calculate the prospective cross section in this channel, we consider the maximal mixing angles constraint from leptonic Higgs channel, as discussed in [32, 33]. While the Higgs bound is most stringent in a large N mass range, at N mass between 100-110 GeV, the EWPD bound [28] becomes stronger. We use the stronger of the two constraints to produce an upper bound of $|V_{lN}|^2$, and the heavy neutrino production cross section for the $h+j$ channel.

For the convenience of estimating generic signal rates, we also use showed the signal cross sections at fixed mixing angle values in In Fig. 3. Note that $|V_{\ell N}|^2 = 10^{-5}$ will be nearly

$\mathcal{O}(1)$ magnitude below the constraint obtained in [28, 32, 33] in the SF case[4].

The heavy neutrino will then decay via the SM weak bosons such as W, Z (and h for heavier N). When N is heavier, it can decay to on-shell W and Z bosons. These partial decay widths are given as,

$$\Gamma(N \to \ell W) = \frac{g^2 |V_{\ell N}|^2}{64\pi} \frac{(M_N^2 - m_W^2)^2 (M_N^2 + 2m_W^2)}{M_N^3 m_W^2} \tag{11}$$

and

$$\Gamma(N \to \nu Z) = \frac{g^2 |V_{\ell N}|^2}{128\pi c_w^2} \frac{(M_N^2 - m_Z^2)^2 (M_N^2 + 2m_Z^2)}{M_N^3 m_Z^2} \tag{12}$$

respectively. When the heavy neutrino mass is greater than the Higgs boson mass, then it can decay into the Higgs boson through at a partial width,

$$\Gamma(N \to h\nu) \;=\; \frac{|V_{\ell N}|^2 (M_N^2 - m_h^2)^2}{32\pi M_N} \left(\frac{1}{v}\right)^2 . \tag{13}$$

For N lighter than W and Z bosons, it decays into three-body channels through the virtual W and Z bosons. The corresponding partial decay widths are

$$\begin{aligned}
\Gamma(N \to \ell_1 \ell_2 \nu_{\ell_2}) &= \frac{|V_{\ell N}|^2 G_F^2 M_N^5}{192\pi^3} \\
\Gamma(N \to \nu_{\ell_1} \ell_2 \ell_2) &= \frac{|V_{\ell N}|^2 G_F^2 M_N^5}{96\pi^3} \Big(\frac{1}{4} + 3\sin^4\theta_w - \frac{3}{2}\sin^2\theta_w\Big) \\
\Gamma(N \to \nu_{\ell_2} \ell_2 \ell_2) &= \frac{|V_{\ell N}|^2 G_F^2 M_N^5}{96\pi^3} \Big(\frac{1}{4} + 3\sin^4\theta_w + \frac{3}{2}\sin^2\theta_w\Big) \\
\Gamma(N \to \nu_{\nu_1} \nu_2 \nu_2) &= \frac{|V_{\ell N}|^2 G_F^2 M_N^5}{96\pi^3} \\
\Gamma(N \to \ell j j) &= \frac{|V_{\ell N}|^2 G_F^2 M_N^5}{64\pi^2} \\
\Gamma(N \to \ell j j) &= \frac{|V_{\ell N}|^2 G_F^2 M_N^5}{32\pi^3} \Big(\frac{1}{4} + 3\sin^4\theta_w - \frac{3}{2}\sin^2\theta_w\Big).
\end{aligned} \tag{14}$$

and these are comparable to [49] where $G_F = 1.166 \times 10^{-5}\text{GeV}^{-2}$.

Note that the W channel will typically dominate both two-body and three-body N decay. In our final state analysis, we require reconstruction of the W boson and N masses to veto SM backgrounds, thus the two-body decay $N \to \ell W$ followed by $W \to jj$, as shown in Fig. 4, is the most relevant channel in the following discussions.

[4] The FD case for the 'benchmark' mixing angles will be nearly twice as large as the corresponding SF cases.

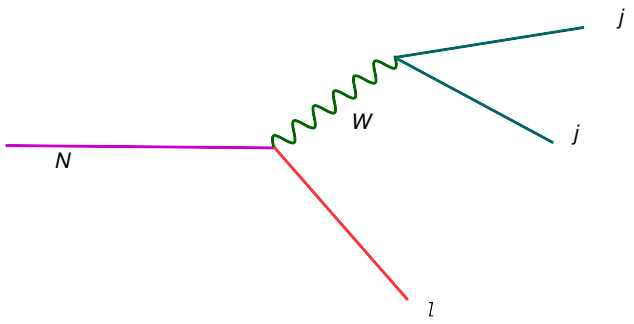

FIG. 4: Decay of the heavy neutrino in the ℓjj mode through the W boson.

IV. COLLIDER SIGNALS AND BACKGROUNDS

For successful triggering and background suppression, we require the leading jet p_T^j in $pp \to hj$ event to be at least 200 GeV. Compared to Higgs boson decay products, the ISR jet is more energetic and assumes the role of triggering jet, and at the same transversely boosts the Higgs boson system so that the Higgs boson decay products acquire larger p_T^j and become more visible.

The Higgs boson then can decay into an $N - \nu$ pair. We focus on the semileptonic N decay channel $N \to \ell jj$, in which all three daughter particles are visible. The two jets from N arises from the on-shell decay of a W boson, so that their invariant mass would reconstruct to M_W. The lepton + dijet invariant mass would also reconstruct to M_N. These two invariant mass window cuts greatly suppress SM backgrounds.

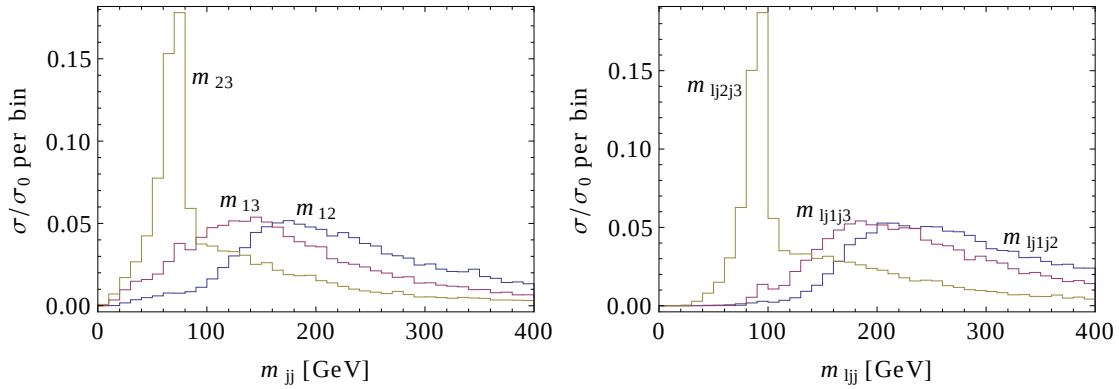

FIG. 5: Invariant dijet (left) and lepton+dijet (right) masses out of the three jets in signal events. N ($M_N = 100$ GeV) decay jets are mostly represented by j_2 and j_3. In these histograms, the signal events only assume selection cuts $N_j \geq 3$ and $N_\ell \geq 1$.

As the ISR jet is often more energetic than those from N decays, the N decay jets are mostly the second and third in p_T^j ordering, as illustrated in Fig. 5. An M_W peak is the

most statistically pronounced between j_2 and j_3 among the three leading jets.

The after-cut cross-section is inferred from the $pp \to hj$ cross-section, decay branching ratios, and the selection efficiencies, as

$$\sigma = \sigma(hj)\mathcal{B}_{h\to N\nu}\mathcal{B}_{N\to \ell jj}A_{\rm eff}. \tag{15}$$

For the selection efficiency $A_{\rm eff}$, we consider the following cuts on the event final state:

(1) leading jet p_T >200 GeV;

(2) Additional two or more jets with $p_T > 30$ GeV and exactly one lepton with $p_T > 15$ GeV;

(3) $|M(j_2 j_3) - M_W| < 20$ GeV;

(4) $|M(l_1 j_2 j_3) - M_N| < 20$ GeV.

The selection cuts are designed to reconstruct the characteristic heavy neutrino mass as well as the physical W boson from N decay. The large leading jet p_T^j is important in suppressing weak boson + jets backgrounds. Vetoing a second lepton removes backgrounds with Z bosons. Here we focus on the hadronical W decay in order to reconstruct both the W boson and the N masses. These cuts greatly reduces SM backgrounds while retaining signal events at a much higher acceptance rate. Note that a fully leptonic decay of N can yield more leptons and suffer fewer SM background channels, but it also yields a neutrino and makes it impossible to reconstruct M_N.

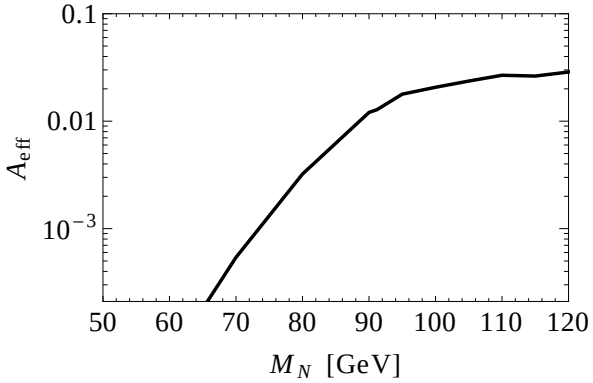

FIG. 6: Accumulative cut efficiency $A_{\rm eff}$ over different heavy neutrino masses. The selection cuts (1)-(4) are imposed on signal event samples that are generated with a leading jet $p_T^j > 100$ GeV.

In order to obtain the cut efficiencies, we perform a Monte Carlo simulation of $pp \to hj$ events with MadGraph5 [50] package and its the Pythia-PGS package for event showering and detector simulation. For basic detector setup, we require a jet pseudo-rapidity $|\eta^j| < 2.5$, lepton pseudo-rapidity $|\eta^\ell| < 2.4$, minimal jet and lepton transverse momenta p_T^j and p_T^ℓ

at 30 GeV and 15 GeV, respectively. Both of ATLAS and CMS handle large number of pile-up interactions using a technique in [46]. We simply use the PGS simulation without pile-up interactions, but jets are in a fiducial volume of tracking system of $|\eta^j| < 2.5$ to remove pile-up interactions. Note that we also choose $|\eta^j| < 2.5$ range to agree with [47] for cross-section scaling.

The cut efficiency for signals is shown in Fig. 6 over the range of M_N. The cut-efficiency is at the level of 1-3% for a N mass between W and h masses. Lighter N has a reduced cut efficiency due to the requirement of M_W reconstruction from $j_2 j_3$. The prospective cross section is given in Fig. 7. The maximally allowed mixing angles from [28, 32, 33] are used. For comparison, we also showed the after-cut cross-section for the 'benchmark' values of $|V_{\ell N}|^2$. 13 TeV the LHC can probe $|V_{\ell N}|^2$ down to 10^{-5} and a corresponding cross section can be readily tested at the future high luminosity LHC runs.

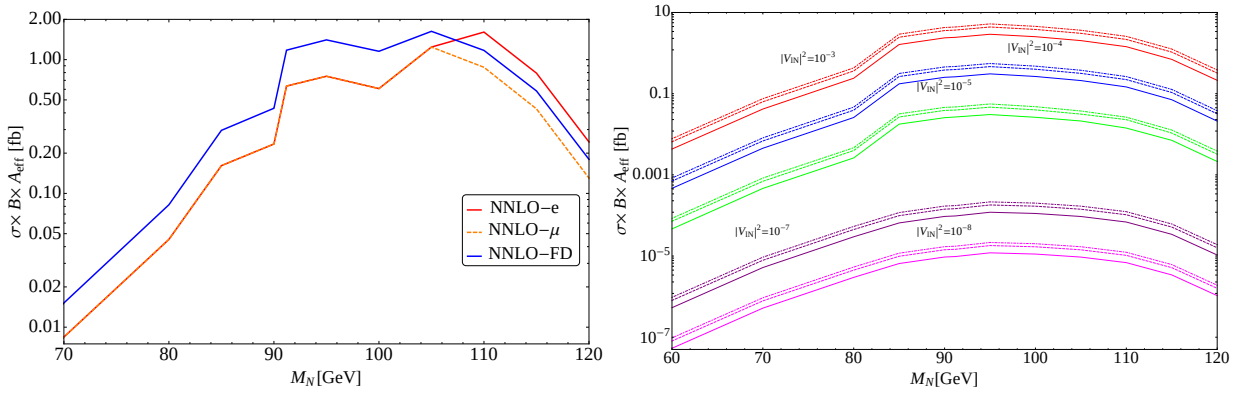

FIG. 7: Similar to Fig. 3 after folding in the efficiency $A_{\rm eff}$ of selection cuts.

Channel	tj	tW	$t\bar{t}$	W+jets	Z+jets	WWj	WZj	ZZj	M_N=100	M_N=105	M_N=110
Pre-cut σ [pb]	40	52	4.7×10^2	2.5×10^3	9.5×10^2	7.1	5.4	0.69	0.017	0.030	0.035
Eff. $p_T(j_1)$>200	0.12	0.034	0.052	0.12	0.13	0.25	0.29	0.23	0.17	0.16	0.17
Eff. $N_j \geq 3, N_l = 1$	0.073	0.14	0.21	0.046	0.014	0.14	0.10	0.039	0.39	0.38	0.48
Eff. $M(j_2 j_3)$ on M_W	0.12	0.16	0.12	0.17	0.14	0.29	0.33	0.27	0.40	0.42	0.40
σ[pb]	0.040	0.038	0.59	2.3	0.24	0.074	0.054	2.0×10^{-3}	3.8×10^{-4}	7.9×10^{-4}	1.0×10^{-3}

TABLE II: Cut efficiencies of Cuts (1)-(3) on SM background and heavy neutrino signals. The 'Pre-cut' cut background cross-sections assume a leading jet p_T >100 GeV cut at event generation level. The W/Z+jets channels are given inclusive cross-section for one to three parton level jets, with jet matching. The other backgrounds are at the leading order. Signal cross-sections assume the ν_e SF case and derive from maximally allowed mixing angles and LO hj cross-section.

A number of SM backgrounds are relevant for the $3j + \ell$ final state. The leading back-

ground channels typically arise from the presence of a W boson, from either direct production or top quark decay, along with ISR jet(s). The significant background channels are listed in Tab. II that shows the efficiencies for the first three cuts, and Tab. III for the final M_N window cut. For signal rates, we list a few N masses between Z and h masses. The mass dependence of $A_{\rm eff}$ is shown in Fig. 6.

As shown in Tabs. II, III, the leading background channel is W+jets, while those with top quarks are efficiently controlled by the N mass-window cut. A large leading jet p_T is the most effective cut against the W+jets channel, but it would also suppress the signal rate. In the Monte-Carlo simulation for the W/Z+jets, we use an 'MLM' matched [51, 52] cross-section for inclusive $V+j, V+jj$ and $V+jjj$ processes, while for the other (sub-leading) background channels, we only showed the leading-order cross-sections.

Mass Window	$\sigma(tj)$	$\sigma(tW)$	$\sigma(t\bar{t})$	$\sigma(W$+jets$)$	$\sigma(Z$+jets$)$	$\sigma(WWj)$	$\sigma(WZj)$	$\lvert V_{\ell N}\rvert^2_{\rm max}$	LO $\sigma_{\rm sig}$	NNLO $\sigma_{\rm sig}$
100	0.011	3×10^{-3}	0.028	0.20	0.022	6.0×10^{-3}	5.0×10^{-3}	3.4×10^{-4}	3.5×10^{-4}	6.1×10^{-4}
105	0.011	4×10^{-3}	0.028	0.23	0.026	8×10^{-3}	6×10^{-3}	9.0×10^{-4}	7.2×10^{-4}	1.2×10^{-3}
110	0.010	6×10^{-3}	0.037	0.23	0.030	9.0×10^{-3}	7.0×10^{-3}	1.7×10^{-3}	9.3×10^{-4}	1.6×10^{-3}

TABLE III: Background cross-sections after the final N mass window cut on invariant mass of the $\ell_1 j_2 j_3$ system. All cross-sections are given in pb. The signal cross-sections and respective maximal mixing assume the ν_e SF case. The W/Z+jets channels are given inclusive cross-section for one to three parton level jets, with jet matching. Other background cross-sections are at the leading order.

After performing all the selection cuts, we found the leading a residue total background cross-section of 0.3 pb for the N masses in Tab. III. The maximal mixing values and corresponding cross-sections are given for the ν_e SF case, for which the EWPD is the least strigent. Adopting the NNLO hj product rate the heavy neutrino signals can be ∼fb in cross-section, thus can be tested at the LHC. Considering the up-coming high luminosity runs at 3000 fb^{-1}, the ν_e SF case $S/\sqrt{B+S}$ ratio is 2.6(3.8) for M_N =100(110) GeV.

The signal cross-section for muon flavor mixing cases can be scaled from Tab. III with the corresponding maximally allowed $|V_{lN}|^2$ values, for relatively small $\mathcal{B}(h\to\nu N)$. In the ν_μ SF case, as the EWPD constrains $|V_{lN}|^2 < 9\times10^{-4}$ for $M_N > 105$ GeV, the signal rates are the same for $M_N < 105$ GeV, but become smaller for heavier M_N.

In the 'FD' case, the EWPD rules the common $|V_{lN}|^2 < 6.3\times10^{-4}$ for $M_N > 105$ GeV, while the combined signal cross-section is enhanced by a factor of 2. The signal optimizes at $M_N = 105$ GeV with a cross-section of 1.6 fb, and for 3000 fb^{-1} luminosity the

$S/\sqrt{B+S} = 5.0$, comparable to the ν_e SF case in signal significance.

A few additional cuts may be considered to help with background control. We note a central region b-jet veto will be effective to reduce the top quark backgrounds, once the W+jets events can be substantially reduced. A requirement of the transverse mass of the $\ell j_2 j_3 \not{E}_T$ system, $M_T(\ell j_2 j_3 \not{E}_T) < M_h$ may further reduce the W+jets background. The effectiveness of these cuts can be further investigated in high-statistics background studies.

As a note, in the ν_τ mixing case the EWPD is less stringent compared to $\nu_{e,\mu}$ mixing cases, but the signal rate suffers from tau identification efficiency, as well as fractional τ energy reconstruction, which can be further studied.

V. CONCLUSION

We investigated the prospect of probing the single-production of a right handed heavy neutrino from the on-shell decay of the SM Higgs boson at the 13 TeV LHC. We adopt the inverted see-saw model where a sizable neutrino mixing angle is allowed. Due to the small SM width of the Higgs boson, a significant $h \to N\nu$ branching ratio can be achieved within the current bounds on the $N\nu$ mixing.

We adopt the maximally allowed $N\nu$ mixing angle, the corresponding Higgs boson decay width, to derive a maximal signal rate for the $pp \to hj$ where the Higgs boson decays into the right-handed neutrino. We require a hard ISR jet to transversely boost the visibility of h, N decay products as well as for background suppression. For N identification, we require both W and N mass reconstruction from the jets and lepton-jet(s) systems in a $3j + \ell$ final state.

A number of kinematical cuts are designed for signal selection. Signal and background analyses are carried out to evaluate the cut efficiencies, as shown in detail in Section IV. We found an cut efficiency at 1-3% for M_N close to Higgs boson mass and a reduced efficiency for lighter N. For a few benchmark N masses 100-110 GeV, a maximal signal cross-section at ∼fb is obtained, compared to a total background at 0.3 pb from various W and t containing background channels. We note that transverse mass cuts may help further rejecting backgrounds. At optimal N masses, the signals in ν_e SF and FD scenarios can be searched for and constrained by the up-coming LHC runs at a signal-to-background ratio around 5 by 3000 fb^{-1} luminosity. The ν_μ SF case has less significance because of stronger EWPD constraints. For N much lighter than the Higgs boson, the signal is much less pronounced

due to reduced decay branching and cut efficiencies.

Acknowledgments

The work AD is supported by the Korea Neutrino Research Center which is established by the National Research Foundation of Korea(NRF) grant funded by the Korea government(MSIP) (No. 2009-0083526). YG thank the Wayne State University for support. TK is partially supported by DOE Grant de-sc0010813. TK is also supported in part by Qatar National Research Fund under project NPRP 9-328-1-066.

---

[1] K. Abe et. al. [T2K Collaboration] Phys. Rev. Lett. 107, 041801 (2011).

[2] P. Adamson et al. [MINOS Collaboration], Phys. Rev. Lett. 107, 181802 (2011).

[3] J. Beringer et. al. [Particle Data Group Collaboration], Phys. Rev. D 86, 010001 (2012).

[4] Y. Abe et al. [DOUBLE-CHOOZ Collaboration], Phys. Rev. Lett. 108, 131801 (2012).

[5] F. P. An et al. [DAYA-BAY Collaboration], Phys. Rev. Lett. 108, 171803 (2012).

[6] J. K. Ahn et al. [RENO Collaboration], Phys. Rev. Lett. 108, 191802 (2012).

[7] P. Minkowski, "$\mu \to e\gamma$ at a Rate of One Out of 10^9 Muon Decays?," Phys. Lett. **67B**, 421 (1977). doi:10.1016/0370-2693(77)90435-X

[8] T. Yanagida, "Horizontal Symmetry and Masses of Neutrinos," Prog. Theor. Phys. **64**, 1103 (1980).

[9] J. Schechter and J. W. F. Valle, "Neutrino Masses in SU(2) $\otimes$ U(1) Theories," Phys. Rev. D **22**, 2227 (1980).

[10] T. Yanagida, in Proceedings of the Work- shop on the Unified Theory and the Baryon Number in the Universe (O. Sawada and A. Sugamoto, eds.), KEK, Tsukuba, Japan, 1979, p. 95.

[11] M. Gell-Mann, P. Ramond, and R. Slansky, Supergravity (P. van Nieuwenhuizen et al. eds.), North Holland, Amsterdam, 1979, p. 315.

[12] S. L. Glashow, The future of elementary particle physics, in Proceedings of the 1979 Carg'ese Summer Institute on Quarks and Leptons (M. Levy et al. eds.), Plenum Press, New York, 1980, p. 687.

[13] R. N. Mohapatra and G. Senjanovic, "Neutrino Mass and Spontaneous Parity Violation," Phys. Rev. Lett. **44**, 912 (1980).

[14] R. N. Mohapatra, Phys. Rev. Lett. 56 (1986) 561.

[15] R. N. Mohapatra and J. W. F. Valle, Phys. Rev. D 34, 1642 (1986).

[16] M. Malinsky, T. Ohlsson, Z. z. Xing and H. Zhang, "Non-unitary neutrino mixing and CP violation in the minimal inverse seesaw model," Phys. Lett. B **679**, 242 (2009) doi:10.1016/j.physletb.2009.07.038 [arXiv:0905.2889 [hep-ph]].

[17] I. Gogoladze, N. Okada and Q. Shafi, "NMSSM and Seesaw Physics at LHC," Phys. Lett. B **672**, 235 (2009) doi:10.1016/j.physletb.2008.12.068 [arXiv:0809.0703 [hep-ph]].

[18] M. Dittmar, A. Santamaria, M. C. Gonzalez-Garcia and J. W. F. Valle, "Production Mechanisms and Signatures of Isosinglet Neutral Heavy Leptons in Z^0 Decays," Nucl. Phys. B **332**, 1 (1990). doi:10.1016/0550-3213(90)90028-C

[19] A. Das and N. Okada, "Inverse seesaw neutrino signatures at the LHC and ILC," Phys. Rev. D **88**, 113001 (2013) doi:10.1103/PhysRevD.88.113001 [arXiv:1207.3734 [hep-ph]].

[20] A. Das, P. Konar and S. Majhi, "Production of Heavy neutrino in next-to-leading order QCD at the LHC and beyond," JHEP **1606**, 019 (2016) doi:10.1007/JHEP06(2016)019 [arXiv:1604.00608 [hep-ph]].

[21] C. Degrande, O. Mattelaer, R. Ruiz and J. Turner, "Fully-Automated Precision Predictions for Heavy Neutrino Production Mechanisms at Hadron Colliders," Phys. Rev. D **94**, no. 5, 053002 (2016) doi:10.1103/PhysRevD.94.053002 [arXiv:1602.06957 [hep-ph]].

[22] A. G. Hessler, A. Ibarra, E. Molinaro and S. Vogl, "Impact of the Higgs boson on the production of exotic particles at the LHC," Phys. Rev. D **91**, no. 11, 115004 (2015) doi:10.1103/PhysRevD.91.115004 [arXiv:1408.0983 [hep-ph]].

[23] O. Adriani *et al.* [L3 Collaboration], "Search for isosinglet neutral heavy leptons in Z0 decays," Phys. Lett. B **295**, 371 (1992). doi:10.1016/0370-2693(92)91579-X

[24] M. Acciarri *et al.* [L3 Collaboration], "Search for heavy isosinglet neutrinos in e^+e^- annihilation at 130-GeV less than $S^{(1/2)}$ less than 189-GeV," Phys. Lett. B **461**, 397 (1999) doi:10.1016/S0370-2693(99)00852-7 [hep-ex/9909006].

[25] P. Achard *et al.* [L3 Collaboration], "Search for heavy isosinglet neutrino in e^+e^- annihilation at LEP," Phys. Lett. B **517**, 67 (2001) doi:10.1016/S0370-2693(01)00993-5 [hep-ex/0107014].

[26] P. Abreu *et al.* [DELPHI Collaboration], "Search for neutral heavy leptons produced in Z decays," Z. Phys. C **74**, 57 (1997) Erratum: [Z. Phys. C **75**, 580 (1997)]. doi:10.1007/s002880050370

[27] A. Blondel *et al.* [FCC-ee study Team], "Search for Heavy Right Handed Neutrinos at the FCC-ee," Nucl. Part. Phys. Proc. **273-275**, 1883 doi:10.1016/j.nuclphysbps.2015.09.304 [arXiv:1411.5230 [hep-ex]].

[28] J. de Blas, "Electroweak limits on physics beyond the Standard Model," EPJ Web Conf. **60**, 19008 (2013) doi:10.1051/epjconf/20136019008 [arXiv:1307.6173 [hep-ph]].

[29] F. del Aguila, J. de Blas and M. Perez-Victoria, "Effects of new leptons in Electroweak Precision Data," Phys. Rev. D **78**, 013010 (2008) doi:10.1103/PhysRevD.78.013010 [arXiv:0803.4008 [hep-ph]].

[30] E. Akhmedov, A. Kartavtsev, M. Lindner, L. Michaels and J. Smirnov, "Improving Electro-Weak Fits with TeV-scale Sterile Neutrinos," JHEP **1305**, 081 (2013) doi:10.1007/JHEP05(2013)081 [arXiv:1302.1872 [hep-ph]].

[31] F. F. Deppisch, P. S. Bhupal Dev and A. Pilaftsis, "Neutrinos and Collider Physics," New J. Phys. **17**, no. 7, 075019 (2015) doi:10.1088/1367-2630/17/7/075019 [arXiv:1502.06541 [hep-ph]].

[32] P. S. Bhupal Dev, R. Franceschini and R. N. Mohapatra, "Bounds on TeV Seesaw Models from LHC Higgs boson Data," Phys. Rev. D **86**, 093010 (2012) doi:10.1103/PhysRevD.86.093010 [arXiv:1207.2756 [hep-ph]].

[33] A. Das, P. S. Bhupal Dev and N. Okada, "Direct bounds on electroweak scale pseudo-Dirac neutrinos from $\sqrt{s} = 8$ TeV LHC data," Phys. Lett. B **735**, 364 (2014) doi:10.1016/j.physletb.2014.06.058 [arXiv:1405.0177 [hep-ph]].

[34] S. Chatrchyan *et al.* [CMS Collaboration], "Search for the standard model Higgs boson decaying to W^+W^- in the fully leptonic final state in pp collisions at $\sqrt{s} = 7$ TeV," Phys. Lett. B **710**, 91 (2012) doi:10.1016/j.physletb.2012.02.076 [arXiv:1202.1489 [hep-ex]].

[35] CMS Collaboration [CMS Collaboration], "Search for the standard model Higgs boson decaying to a W pair in the fully leptonic final state in pp collisions at sqrt(s) = 8 TeV," CMS-PAS-HIG-12-017.

[36] G. Aad *et al.* [ATLAS Collaboration], "Search for the Standard Model Higgs boson in the $H \to \mathrm{WW}^* \to \ell\nu\ell\nu$ decay mode with 4.7 /fb of ATLAS data at $\sqrt{s} = 7$ TeV," Phys. Lett. B **716**, 62 (2012) doi:10.1016/j.physletb.2012.08.010 [arXiv:1206.0756 [hep-ex]].

[37] S. Chatrchyan *et al.* [CMS Collaboration], "Search for the standard model Higgs boson in the H to ZZ to 2 $\ell 2\nu$ channel in pp collisions at $\sqrt{s} = 7$ TeV," JHEP **1203**, 040 (2012) doi:10.1007/JHEP03(2012)040 [arXiv:1202.3478 [hep-ex]].

[38] G. Aad *et al.* [ATLAS Collaboration], "Search for a standard model Higgs boson in the $\mathrm{H} \to \mathrm{ZZ} \to \ell^+\ell^-\nu\bar{\nu}$ decay channel using 4.7 fb^{-1} of $\sqrt{s} = 7$ TeV data with the ATLAS detector," Phys. Lett. B **717**, 29 (2012) doi:10.1016/j.physletb.2012.09.016 [arXiv:1205.6744 [hep-ex]].

[39] S. Banerjee, P. S. B. Dev, A. Ibarra, T. Mandal and M. Mitra, "Prospects of Heavy Neutrino Searches at Future Lepton Colliders," Phys. Rev. D **92**, 075002 (2015) doi:10.1103/PhysRevD.92.075002 [arXiv:1503.05491 [hep-ph]].

[40] [ATLAS Collaboration], "Search for Majorana neutrino production in pp collisions at $\sqrt(s) = 7$ TeV in dimuon final states with the ATLAS detector," ATLAS-CONF-2012-139; S. Chatrchyan *et al.* [CMS Collaboration], "Search for heavy Majorana neutrinos in $\mu^{\pm}\mu^{\pm}$+ jets and $e^{\pm}e^{\pm}$+ jets events in pp collisions at $\sqrt{s} = 7$ TeV," Phys. Lett. B **717**, 109 (2012) doi:10.1016/j.physletb.2012.09.012 [arXiv:1207.6079 [hep-ex]].

[41] G. Aad *et al.* [ATLAS Collaboration], 'Search for heavy Majorana neutrinos with the ATLAS detector in pp collisions at $\sqrt{s} = 8$ TeV," JHEP **1507** (2015) 162 doi:10.1007/JHEP07(2015)162 [arXiv:1506.06020 [hep-ex]].

[42] V. Khachatryan *et al.* [CMS Collaboration], "Search for heavy Majorana neutrinos in $e^{\pm}e^{\pm}$+ jets and $e^{\pm}$ $\mu^{\pm}$+ jets events in proton-proton collisions at $\sqrt{s} = 8$ TeV," JHEP **1604**, 169 (2016) doi:10.1007/JHEP04(2016)169 [arXiv:1603.02248 [hep-ex]].

[43] A. Das and N. Okada, "Improved bounds on the heavy neutrino productions at the LHC," Phys. Rev. D **93**, no. 3, 033003 (2016) doi:10.1103/PhysRevD.93.033003 [arXiv:1510.04790 [hep-ph]].

[44] A. Das and N. Okada, "Bounds on heavy Majorana neutrinos in type-I seesaw and implications for collider searches," arXiv:1702.04668 [hep-ph].

[45] A. Das, "Pair production of heavy neutrinos in next-to-leading order QCD at the hadron colliders in the inverse seesaw framework," arXiv:1701.04946 [hep-ph].

[46] M. Cacciari and G. P. Salam, "Pileup subtraction using jet areas," Phys. Lett. B **659**, 119 (2008) doi:10.1016/j.physletb.2007.09.077 [arXiv:0707.1378 [hep-ph]].

[47] R. Boughezal, F. Caola, K. Melnikov, F. Petriello and M. Schulze, "Higgs boson production in association with a jet at next-to-next-to-leading order," Phys. Rev. Lett. **115**, no. 8, 082003 (2015) doi:10.1103/PhysRevLett.115.082003 [arXiv:1504.07922 [hep-ph]].

[48] R. Boughezal, C. Focke, W. Giele, X. Liu and F. Petriello, "Higgs boson production in association with a jet at NNLO using jettiness subtraction," Phys. Lett. B **748**, 5 (2015) doi:10.1016/j.physletb.2015.06.055 [arXiv:1505.03893 [hep-ph]].

[49] C. O. Dib, C. S. Kim, K. Wang and J. Zhang, "Distinguishing Dirac/Majorana Sterile Neutrinos at the LHC," Phys. Rev. D **94**, no. 1, 013005 (2016) doi:10.1103/PhysRevD.94.013005 [arXiv:1605.01123 [hep-ph]].

[50] J. Alwall *et al.*, "The automated computation of tree-level and next-to-leading order differential cross sections, and their matching to parton shower simulations," JHEP **1407**, 079 (2014) doi:10.1007/JHEP07(2014)079 [arXiv:1405.0301 [hep-ph]].

[51] S. Mrenna and P. Richardson, "Matching matrix elements and parton showers with HERWIG and PYTHIA," JHEP **0405**, 040 (2004) doi:10.1088/1126-6708/2004/05/040

[52] M. L. Mangano, M. Moretti, F. Piccinini and M. Treccani, "Matching matrix elements and shower evolution for top-quark production in hadronic collisions," JHEP **0701**, 013 (2007) doi:10.1088/1126-6708/2007/01/013 [hep-ph/0611129].